24th COBEM - 2017

24th ABCM International Congress of Mechanical Engineering
December 3-8, 2017, Curitiba, PR, Brazil

COBEM-2017-1437
EXPERIMENTAL PARAMETERS FROM FLUID DYNAMICS AND NATURAL GAS COMBUSTION IN FLUIDIZED BED REACTOR

J. D. M. Feitosa
W. M. Barcellos
diego7mat@yahoo.com.br and william_barcellos@ufc.br

T. S. Pires
tiago.siqueira.pires@gmail.com;

W. C. de Araújo
a.welkson@yahoo.com.br;
L. R. Costa
lucas_rcosta@hotmail.com.br;
T. M. Dantas
thiagomdantas@alu.ufc.br;
F. E. P. Cardoso
fernanda_epc@yahoo.com.br;
K. C. J. B. Ribeiro
engmeckaique@gmail.com;
M. C. D'Amico
marco.mcd@gmail.com;
J. W. C. de Araújo
Laboratory of Combustion and Renewable Energies. Department of Mechanical Engineering – Federal University of Ceará.
Fortaleza, Ceará, Brazil - 60.455-970
a.welbson@gmail.com.

Abstract: *Gaseous fluidization of solid particles has been applied to the burning not only of natural gas (NG) but also of different kinds of fuels, including solid biomass, leading to low pollutant emission rates. In this context, this paper presents experimental results from studies about fluid dynamic and NG combustion in fluidized bed. Considering a silica particle bed and an airflow crossing its entire length, the main parameters about the gaseous fluidization of the solid phase were identified. The influences of bed diameter and particle size variation on the pressure profile were investigated, utilizing acrylic tubes with different diameters and proper bed heights, which allowed learning about the fluid dynamic phenomena. For a second research step, another study setup was built, using steel tube internally covered with refractory material, normally employed in combustion chambers of industrial boilers, to study the effects of surface roughness on the pressure profile and the minimum fluidization velocity. And, integrating experimental results from fluid dynamic studies with both the setups, a reactor was designed to analyze the combustion process in fluidized bed, specifying a chamber of 550-mm length and 53-mm diameter in which this diameter corresponds to the finest tube with the addition of the wall effects. In the sequence, the reactor was build and instrumented in order to measure pressure and temperature along the bed, which allowed monitoring the combustion process. Using NG as reference fuel, the process of startup was investigated and, on stabilized operation, NOx emissions lower than 10 ppm were obtained, pointing out limitations and particularities of this combustion thermal system.*

Keywords**:** *Fluidized bed, combustion, natural gas, NOx emissions.*

1. INTRODUCTION

Combustion of fossil fuels other than natural gas results in the emission of enormous amounts of compounds and particulates that have negative impacts on human health (EIA, 1999). According to Faramwy, Zaki and Sakr (2016), the natural gas is considered to be an environmentally friendly clean fuel when compared with other fossil fuels (coal and crude oil). Globally, natural gas accounts for 23.7% of primary energy consumption (BP Statistical Review of World Energy, 2015). The expected growth of the global natural gas demands is 1.9% per annum over the BP Energy

Outlook (2015) and usage by the power and industrial sectors accounts for over 80% of the growth in the global demand for natural gas (Faramwy, Zaki and Sakr, 2016).

The global shift from fossil fuel to natural gas for power improves the energy efficiency represents a future of lower carbon emissions (Faramwy, Zaki and Sakr, 2016). The recent shift in policy intentions catalyzed by COP21 is stimulating the much-needed global energy transition giving new momentum to the move toward a lower-carbon and more efficient energy system (Salatino and Solimene, 2017). In this context, the search for cleaner and more efficient ways of power generation have led to an increase on the study of combustion in fluidized bed technologies (Oka, 2004). Some benefits of this technology stand out, such as: the ease to burn and gasify various types of biomass fuels, including gaseous fuels such as Natural Gas; high thermal efficiency associated to low emissions index for SO_2 and NOx (Basu, 2006). Those advantages are related to the presence of a porous media with the capacity of heat transfer by conduction, maintain a uniform reaction zone and low temperatures compared to the conventional technologies (Basu, 2006). According to Sotudeh-Gharebaagh, Chaouki and Legros (1999), at temperatures below 800°C, no thermal NOx is formed and the combustion of gaseous fuel such as natural gas at such temperatures can be considered attractive.

Therefore, combustion of natural gas in fluidized-bed attracted vast amount of attention of the researchers over the years. Sotudeh-Gharebaagh, Chaouki and Legros (1999) studied the natural gas combustion in a turbulent and bubbling fluidized bed of inert particles. Their study provided comprehensive data on gaseous fuel combustion and CO oxidation profile in a pilot plant fluidized bed of inert particles and the experimental results show that the fluidized-bed reactors offer excellent thermal uniformity and temperature control. Zukowski (2003) verified that combustion of premixed natural gas and air in a bubbling fluidized bed of inert particles of sand does not take place throughout the volume of the bed, but is concentrated at a certain distance from the distributor and this location of combustion affects the composition of the gases leaving the bed. For excess air 40% and flow rate 1.66 dm³/s, the NOx emissions was 7 ppm. Dounit, Hemati and Andreux (2008) presented a theoretical and experimental study of natural gas–air mixture combustion in a fluidized bed of sand particles, realizing that dense bed temperature, the fluidizing velocity and the mean particle diameter significantly have affect the thermal behaviors. The natural gas combustion modelling proposed by Pré and Hémati (1998) was used to predict the reactor dense region while the Kunii and Levenspiel (1990) modelling was used to describe the freeboard region. Besides, two-stage kinetic scheme of methane conversion proposed by Dryer and Glassman (1973) was used. These models provided a good representation of the experimental data.

On the other hand, some authors have worked on modeling combustion in fluidized bed applying Computational Fluid Dynamics -CFD as tools to study combustion process phenomena. Singh, Brink and Hupa (2013) presented a modeling to study combustion and gasification of fuels in fluidized bed devices. They have mentioned that CFD has played an active part in analysis of the distribution of products, heat flux, flow, temperature, ash deposits, CO, SOx and NOx emissions during combustion and gasification of fuels in fluidized bed. According to them, the CFD model results have been satisfactory and have made good agreements with the experimental data in many cases, however, the simulations still have many approximate models as well as some assumptions. Recently, the fluidization and heat transfer behaviors of a bubbling fluidized bed were studied by Ngoh, Wee and Lim (2016) using CFD in which the simulations were conducted with varying particle sizes and inlet gas superficial velocities. Solid volume fraction, solid temperature, air temperature, solid velocity vectors, and air velocity vectors distributions were analyzed and compared for various operating conditions.

According to Singh, Brink and Hupa (2013) there are many aspects of fluidized beds where the application of CFD modeling still needs to be explored, thus, to ensure CFD simulations are more than just theoretical exercises, more experimental studies are needed. Based on Bisognin, J. M. Fusco, C. Soares (2016), despite the several researches and the several uses of fluidized beds, engineers and researchers still encounter challenges in their modeling and scale up because the complex phenomena that occurring inside fluidized beds are still not completely understood. In this way, it is interesting to investigate more experimentally the combustion of the natural gas in the fluidized bed and the fluid dynamics phenomena present in the process.

The main objective of this article is the experimental investigation of the operation and design parameters that can influence the fluid dynamics and the combustion process in fluidized bed, such as: particle size, bed diameter, bed height, surface roughness and bed temperature. In addition, details about the startup of the fluidized bed reactor (FBR) and NOx emissions were analyzed, using natural gas (NG) as reference fuel.

2. FUNDAMENTALS OF FLUID DYNAMICS IN FLUIDIZED BED

According to Geldart (1986), the pressure drop across the bed depends only on the mass of the particle bed (M) and the cross-sectional area of the bed (A_t) and can be calculated by the equation:

$$\Delta P_f = \frac{M \cdot g}{A_t} = L_{mf} \cdot (\rho_p - \rho_f) \cdot (1 - \varepsilon_{mf}) \cdot g \tag{1}$$

Where g is the local gravity acceleration, ε_{mf} is the minimum fluidization porosity, L_{mf} is the bed height at the incipient velocity (measured from the air distributor to the bed surface), ρ_p e ρ_f are the specific masses of the particle and fluid, respectively. For the study of the fluidized bed, it is necessary to define some physical properties of the bed of solid particles, such as porosity and bed specific mass. The most widely used method to evaluate the fluidization of particles is the Ergun equation (1952), which is quoted below:

$$\frac{\Delta p}{L} = 150 \cdot \frac{(1-\varepsilon)^2}{\varepsilon^3} \cdot \frac{\mu_f \cdot u}{d_{SV}^2} + 1.75 \cdot \frac{(1-\varepsilon)}{\varepsilon^3} \cdot \frac{\rho_f \cdot u^2}{d_{SV}} \tag{2}$$

Where the sphericity (ϕ_S) is defined as the ratio of the surface area of a sphere having a volume equivalent to the particle and the surface area of the particle and d_{SV} is the characteristic diameter of the particle, given by the product of the sphericity of the particle and the diameter d_V (the diameter of a sphere having the same volume as the particle).

An important number for the characterization of the fluidization conditions is the Reynolds number of the particle (Re_p) used to classify the flow as laminar or turbulent. As Geldart (1986) points out under laminar flow conditions ($Re_p < 1$) the first term on the right side of Equation (2) is dominant and the second term can be eliminated in the same way for completely turbulent regime conditions ($Re_p < 1000$) the second term of Equation (2) is dominant and so the first term can be neglected. The Reynolds number of the particle is given using d_{sv}.

Combining Equation (1) with Equation (2) in the conditions of minimum fluidization has:

$$\frac{\rho_f \cdot d_{SV}^3 \cdot (\rho_p - \rho_f) \cdot g}{\mu_f^2} = \frac{150 \cdot (1-\varepsilon_{mf})}{\varepsilon_{mf}^3} \cdot \frac{\rho_f \cdot d_{SV} \cdot u_{mf}}{\mu_f} + \frac{1.75}{\varepsilon_{mf}^3} \cdot \frac{\rho_f{}^2 \cdot d_{SV}^2 \cdot u_{mf}^2}{\mu_f^2} \tag{3}$$

3. EXPERIMENTAL APPARATUS AND PROCEDURES

The experimental work was carried out using two test apparatus, in order to understand the phenomena of the gas fluidization process inside a reactor, filled with silica particles, and to find out the operation and design parameters. However, the experimental study was carried out in three stages using these two test setups, as follows: i) Laboratory setup equipped with three acrylic tubes of different internal diameters (0.044 m, 0.065 m and 0.090 m), performing fluid dynamics studies at the environment temperature; ii) This same setup adapted with the replacement of acrylic tube by steel tube with internal wall of refractory concrete, performing fluid dynamics studies at different temperatures; iii) Using another experimental apparatus, where a reactor was developed and installed based on the data from the first two stages, also constructed of steel with internal wall of refractory concrete (bed diameter of 0.053 m), so that the combustion study with NG in fluidized bed can be performed. Respectively, the experimental apparatus used in the first two steps is shown in Figure 1 and the apparatus of the third step is shown in Figure 2.

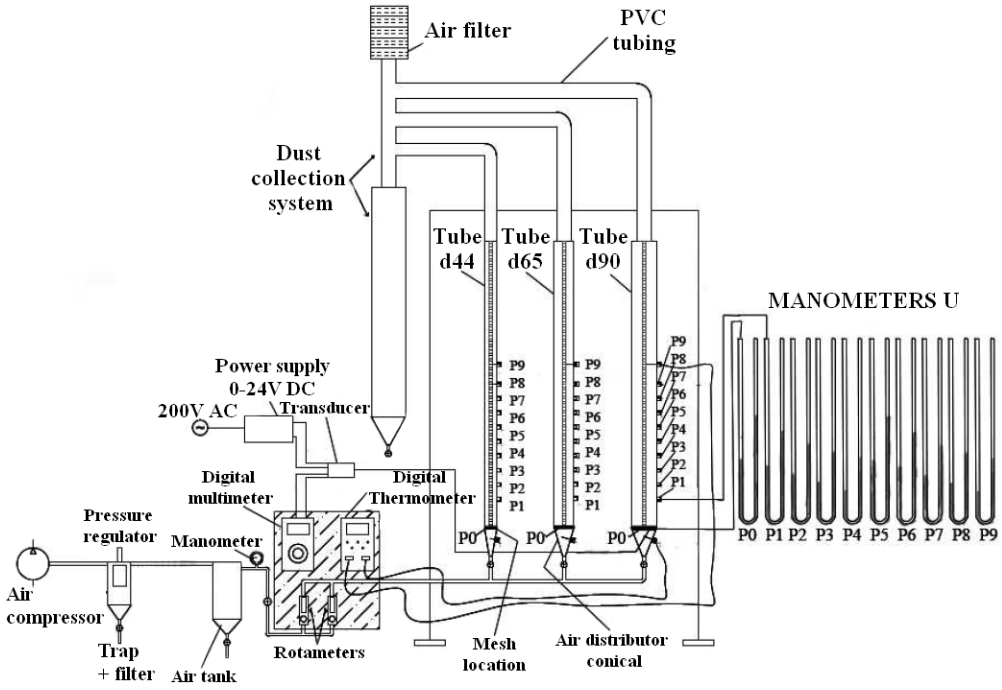

Figure 1. Diagram of the Experimental Apparatus I to fluid dynamic studies with acrylic tubes

The fluid dynamic experimental study of the first stage was carried out in a bed of silica particles (beach sand) to investigate the influence of the following factors: bed diameter, particle size, initial bed height. For this, in each tube several lateral holes were done to allow the reading of pressure in different heights of the bed, being possible to investigate the pressure profile during the fluidization. The pressure measurement positions at the tube side used in the studies were: 0.100 m, 0.150 m, 0.200 m, 0.250 m, 0.300 m, 0.350 m, 0.400 m and 0.500 m. About the silica particle size, three averaged particle diameters were used: 546 μm, 321 μm and 72 μm.

In Fig. 1, the designations P0, P1, P2, P3, P4, P5, P6, P7, P8 and P9 represent the pressure measurement position so that the measurement at the base (P0) and at the sides were carried out by manometers of type U with a measuring range between 0 and 1000 mm of H2O column. In addition, for guarantying the pressure measures with manometer U, a piezo-resistive sensor (Kistler brand, model 4618A0) was used, measuring the absolute pressure at the bed base, to calibrate and validate the measurements performed. Air-fuel mixture flows were controlled to identify the minimum fluidization velocity of the solid phase as well as process temperatures were controlled by thermocouples installed along and after the bed.

Based on the experimental results obtained in the first step, the effects of granulometry could be reasonably known. For this reason, the second and third stages of the experimental study were carried out with particles of mean diameter of 546 μm, due to their greater economic viability. It is worth mentioning that the test methodology was the same in each fluid dynamics study, for both the experimental apparatuses, maintaining all the parameters and varying the influence factors. In this context, the factors considered influential in the fluidization process were the roughness of the inner wall of the tube surrounding the bed and the average temperature of the silica bed. For this reason, the best bed height to be used in the combustion experiments in the reactor was obtained through fluid-dynamic tests at room temperature with the concrete-coated steel pipe with internal diameter of 0.053 m and internal length of 0.550 m, considering the effects of walls.

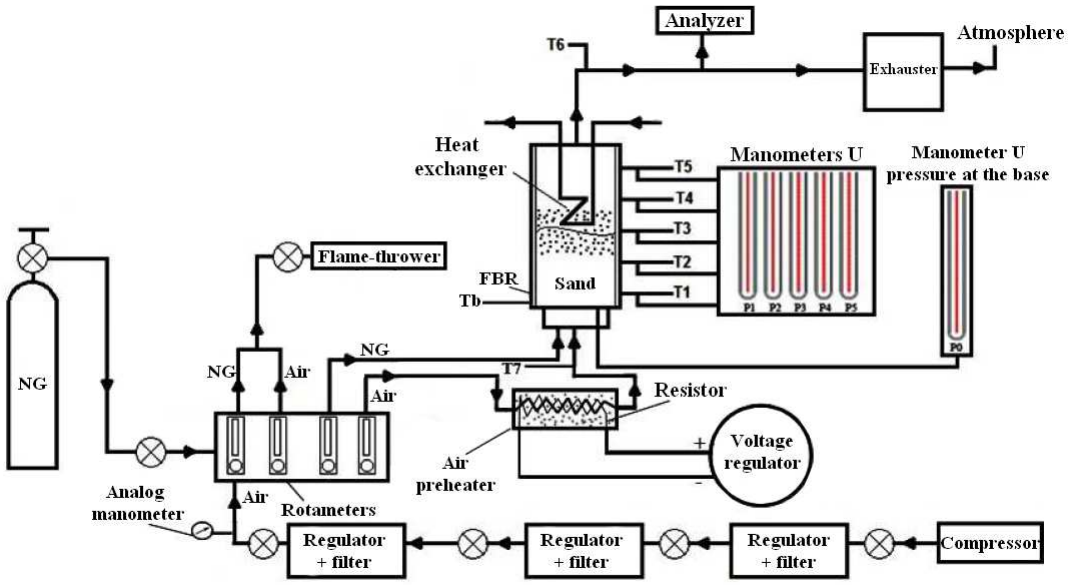

Figure 2. Diagram of the Experimental Apparatus II to fluid dynamic and combustion studies on a fluidized bed reactor

With base on that, several tests were performed varying the bed temperatures to investigate the influence of temperature in the fluidization process. For the investigation of the influence of temperature, the bed was heated by a flamethrower installed in the upper part of the bed and thus the fluidization process was started for different average temperatures of the bed. The heating process to reach the optimum startup temperature revealed that it occurred faster than the initiation of the reactor performed with used electrical resistances previously. Thus, it was possible to investigate the variation of the pressure profile as a function of different bed temperatures and to observe how this affected the minimum fluidization velocity. In the third stage, dedicated to the combustion study with NG, a reactor was developed through of knowledge acquired with the before two setups. In this last experimental apparatus, the startup of the combustion process in the bubbling fluidized bed was investigated and the NOx emissions were analyzed. The tests also indicated that it is interesting to fluidize the bed previously to avoid the exaggerated compaction due to the thermal dilation of silica. In principle, the temperature of 1200 ° C was adopted as that required at the startup. From that

moment, the flamethrower was turned off and the behavior of the temperature distribution profile over time was analyzed as well as the NOx emissions.

4. RESULTS AND DISCUSSIONS

With the objective of validating the experiments with simpler sensors, manometers type "U", a precision piezo-resistive sensor was used for a comparative analysis of the results. The Fig. 3 shows the results of experimental data over the pressure drop across the bed in function of the superficial air velocity used to fluidize the sand in an acrylic tube, as it can be seen in Moreira, et al. (2013). The curves in this graph present a characteristic fluidization profile and it can be observed that the results measured with the "U" manometer and the piezo-resistive manometer are close. This fact validates the measures made by the "U" manometers. The experiments were made for the following conditions: Mean diameter particle of 546 µm, starting bed height of the bed of 0.425 m, bed diameter of 0.090 m, bed temperature at 27 °C. The curves are designated as ΔP-upward and ΔP-downward representing the values obtained during the increment and the decrement of air velocity during the fluidization, respectively, for both pressure sensors, that were installed on the base of the sand bed. A striking characteristic of fluidization of solid particles is the difference of the gauge pressure between the increase and decrease of superficial velocity, this phenomenon occurs when the bed is initially compacted, as points Geldart (1986), which characterizes the hysteresis phenomenon. In addition, it should be emphasized that the peak values of pressure drop tend to be bigger as the bed compaction increases.

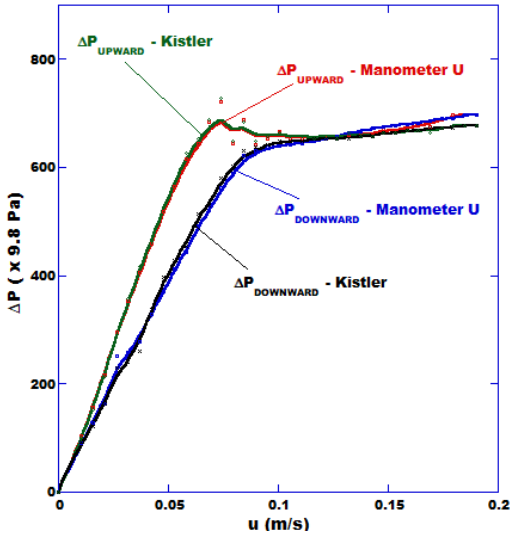

Figure 3. Graph of pressure gauge calibration ΔP x u - Upward and Downward.

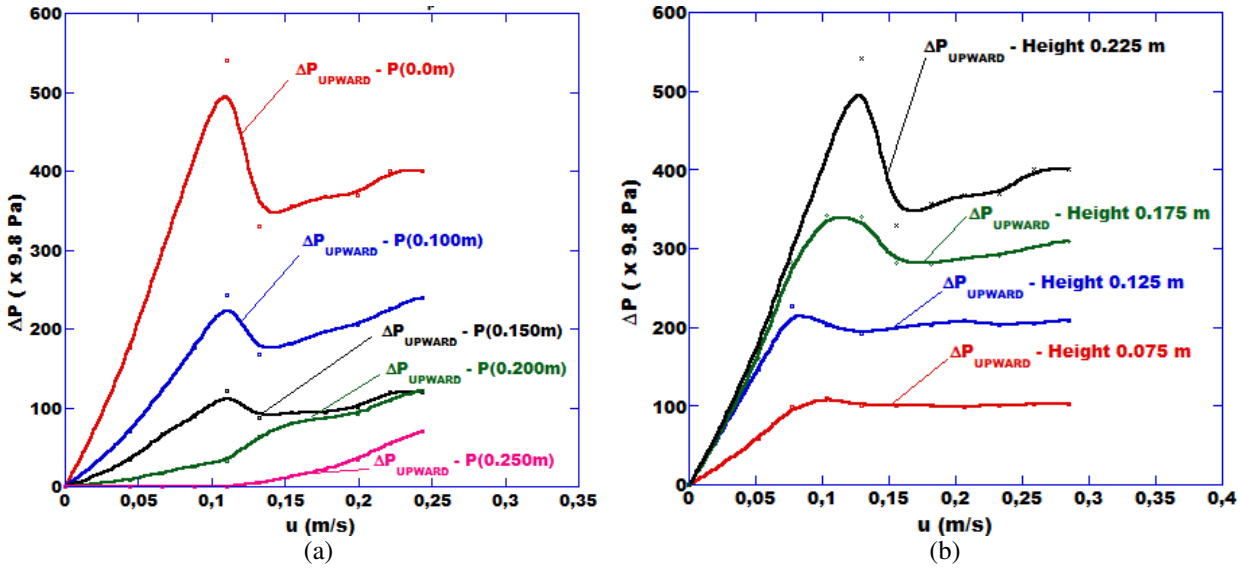

(a) (b)

Figure 4: (a) Graph of pressure profile ΔP x u on different measurement points, ϕ=0.044 m (Upward).
(b) Graph of pressure profile ΔP x u to different bed heights, ϕ=0.044 m (Upward).

Figure 4 (a) shows bed pressure drop measures during the fluidization velocity increase of the air. In these graphics it is possible to observe how the pressure variation occurs along the bed column. The conditions set in test of these graphics were: bed diameter (ϕ) of 0.044 m, silica with particle diameter (Dp) of 546 µm, initial bed height of 0.225 m and bed average temperature in 27 °C. As can be seen, the gauge pressure values along the bed decreases as the pressure measurement point moves away from the bottom, hence, approaching the bed surface. This behavior of the gauge pressure variation throughout the bed occurs similarly to all diameters studied: 0.044 m, 0.065 m, 0.090 m, as was also observed by Moreira, et al. (2013). Based on the velocity increment curves shown in Fig. 4 (a), the highest pressure peak due to the bed compaction occurs for the curves closest to the base "ΔP_{upward} – P(0.0 m), P(0.100 m), P(0.150m)". However, the gauge pressure curves performed by the sensors closest to the surface do not show the peak, which can be evidenced by the small amount of particles above these measure points and by the smaller compaction of the regions closer to the surface "ΔP_{upward} – P(0.200 m) and P(0.250 m)."

Figure 4 (b) presents bed gauge pressure measures for different fluidization velocities during the increase of air velocity. The conditions set in these experiments was: bed diameter (ϕ) of 0.044 m, mean particle diameter of the sand (Dp) of 546 µm, pressure measurement with sensor at 0.0 m from the base and average bed temperature at 27 °C. Comparing the incremental curves of the tests of Fig. 4 (a) and (b) it is possible to observe the similarity of the pressure drop distribution profiles, wherein these graphs represent, respectively, measures taken at the base and along the bed maintaining a fixed height of silica and measures taken only in the base varying the bed height. Still, from the Fig. 4 (b), it can be noticed that the curves that presented higher values of pressure correspond to those with higher initial mass of bed, that is, greater height. Besides that, it was possible to identify the stability of the bubbling fluidized bed regime, evidenced by the region after the maximum pressure peak with approximately constant values as the fluid velocity increases. It is worth mentioning that for higher bed heights, the bubbling regime range tends to be reduced, repeating this phenomenon in all bed diameters studied. This phenomenon, in a way, signals an interesting design parameter for the design of combustion reactors in bubbling fluidized bed, where a stable regime is required to maintain the combustion process.

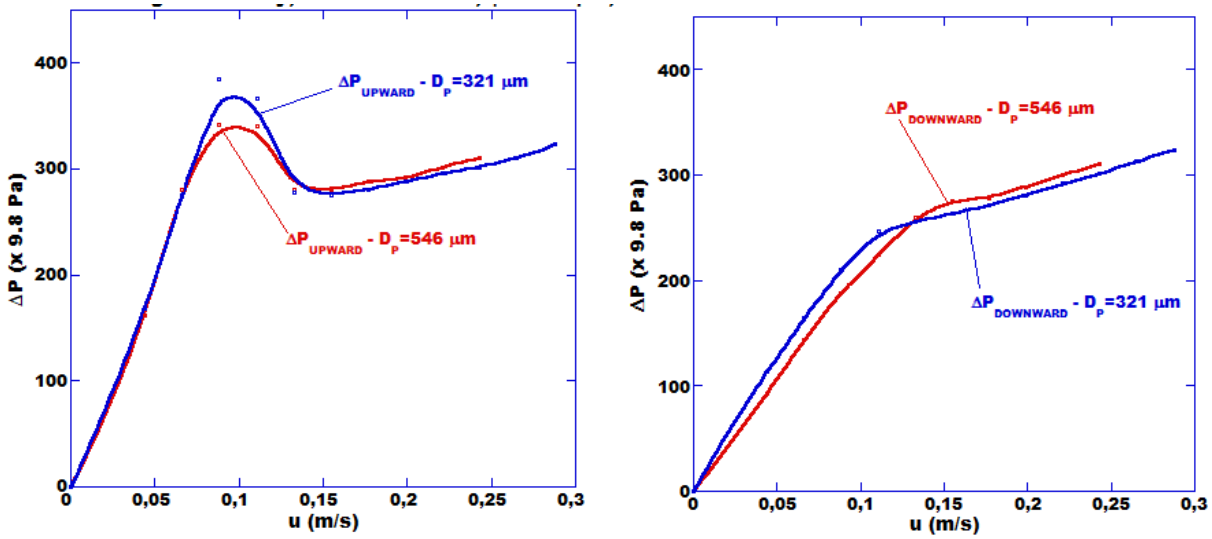

(a) (b)

Figure 5: (a) Graph of pressure profile ΔP x u to different mean particle diameter, ϕ=0.044 m (Upward). (b) Graph of pressure profile ΔP x u to different mean particle diameter, ϕ=0.044 m (Downward).

The curves of Fig. 5 (a) and (b) represent the pressure drop profiles as a function of the velocity used in the fluidization during the increase and the decrease, respectively. The tests of these graphs were performed under the following conditions: bed diameter (ϕ) of 0.044 m, pressure measurement made with the sensor at the bed base, initial bed height of 0.175 m and mean bed temperature of 27 ° C. These initial conditions were maintained during different tests, while measuring the pressure for the granulometry of 546 µm and 321 µm. Through these experiments, it was observed a great similarity between the fluidization curves, both during the increase and decrease of air flow. These results may show the viability of using relatively bigger mean particles diameter, which would be profitable as the silica with smaller mean diameter of particle needs, many times, to pass through costly milling and classifying processes. Tests employed using bigger bed diameters have also presented this similar characteristic, however this was not as important as the presented for smaller bed diameters. These results, that confirms the similarity profiles of gauge pressure for 546 µm and 321 µm on the 0.090 m of bed diameter, can be seen in Moreira, et al. (2013). This aspect besides of validating the diameter specification of particle to fill the reactor, presents itself as an interesting factor for the reduction of operational cost.

In order to characterize an influence of the bed diameter on the fluidization, the data obtained from experimental studies of Moreira, et al. (2013), are being used in this paper, and are displayed by means of Fig. 6 (a), since it is an important parameter of design of fluidized bed reactors. Where the graph of Fig. 6 (a) represents as curves during the increase of air flow. The experimental conditions of the tests were: initial bed height of 0.175 m, sensor pressure measurement at 0.0 m from the base, mean particle size of 546 m and average bed temperature at 27 °C. It should be noted that these conditions are maintained in different tests while performing a pressure measure for different bed diameters. As can be seen from the graphs of Figure 6 (a), a region corresponding to the fixed bed regime, characterized by the initial linearity of the graph, has different positions corresponding to the respective bed diameters, where larger slopes relative to the abscissa axis were obtained for smaller diameters. Another important aspect is the fact of the diameters closest to a region of bubbling fluidized regime more stable than in smaller diameters. This characteristic is evidenced by the narrowing of the region of bubbling regime, approximately constant range after a fluidization of the sand particles. Such reduction of the bubbling regime range can be better characterized by the increment curve corresponding to the diameter of 0.044 m. In addition, a lower operating range under a bubbling regime, a lower fluidization stability was obtained because in a few flow or bed increments the bubbling and turbulent transition regime, i.e., slugging, was triggered more quickly. This more unstable regime, with bubbles next to the bed diameter, is displayed on the graph by the steep slope of the "ΔP_{upward} - ϕ = 0.044 m" curve, just after the bubbling fluidization regime (constant region after minimal fluidization).

As for the investigation, in the experimental apparatus II, to identify the influence of the wall effects on the gaseous fluidization behavior of the solid phase, data are presented through Figure 6 (b) for comparison with the results obtained with the acrylic tubes. The graphs of this figure present the results of fluid dynamics tests for the 0.053 m internal diameter reactor, such that the test conditions are similar to the conditions of the experiments of Fig. 4 (b). Despite the different internal diameter and different wall roughness, the results were similar and are evident when comparing increment curves of the graphs of Figures 6 (b) and 4 (b). In the same way as for the tests performed with the acrylic tubes, the experiments performed with the inner wall bed of refractory material presented higher stability and bubbling fluidization regime range for lower initial bed heights. While for greater heights, a narrowing of this band and the formation of “slugs” occurred for smaller speeds.

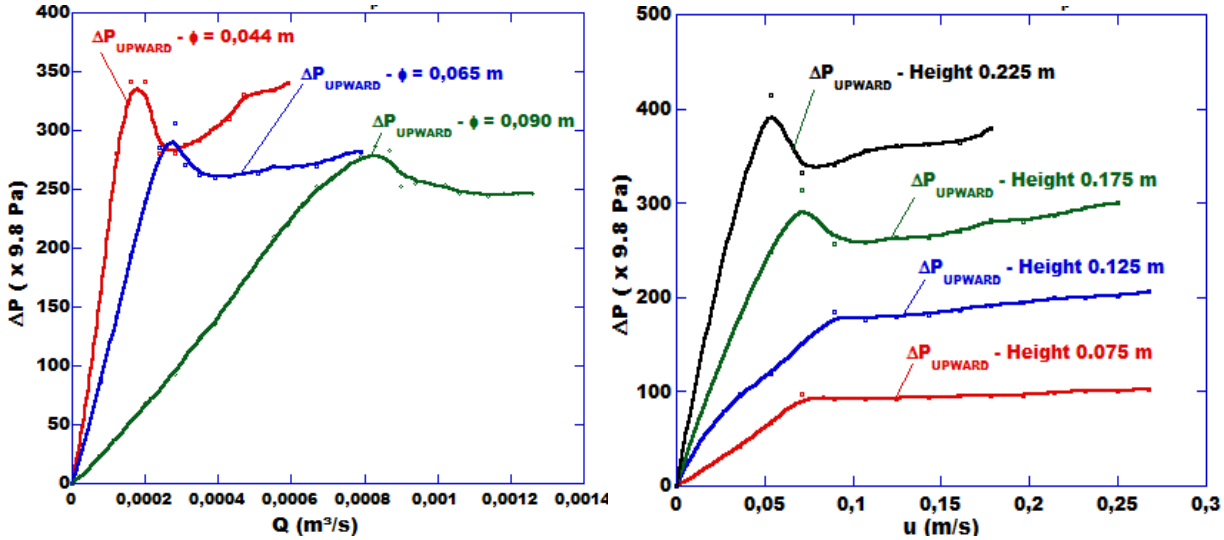

(a) (b)

Figure 6: (a) Graph of pressure profile ΔP x Q to different bed diameters, Dp = 546 µm (Upward).
(b) Graph of pressure profile ΔP x u to different bed heights, ϕ=0.053 m (Upward).

The graph of Fig. 7 (a) shows, in addition to the results presented in Figure 6 (a), the curve of the experiment performed with the internal wall reactor of refractory material with internal diameter of 0.053 m and the curve corresponding to the expected fluidization behavior in an acrylic tube with a diameter of 0.053 m. It is worth mentioning that due to the difficulty of obtaining an acrylic tube with such diameter, an interpolation method was used for this comparative analysis. As can be observed, the curves of the pressure drop profiles as a function of the air flow for the acrylic tube with a diameter of 0.044 m presents inclination and behavior similar to the curve referring to the reactor of refractory material with a diameter of 0.053 m. As can be seen in more detail in Fig. 7 (b), after the fluidization, the same inclination trend was also maintained during the bubbling and slugging regime. This behavior, which indicates an influence of the roughness of the inner wall of the bed due to the increased friction between the particles and the inner walls, justifies the pressure profiles to the smoother tube relative to the rough tube of larger diameter have similar configurations.

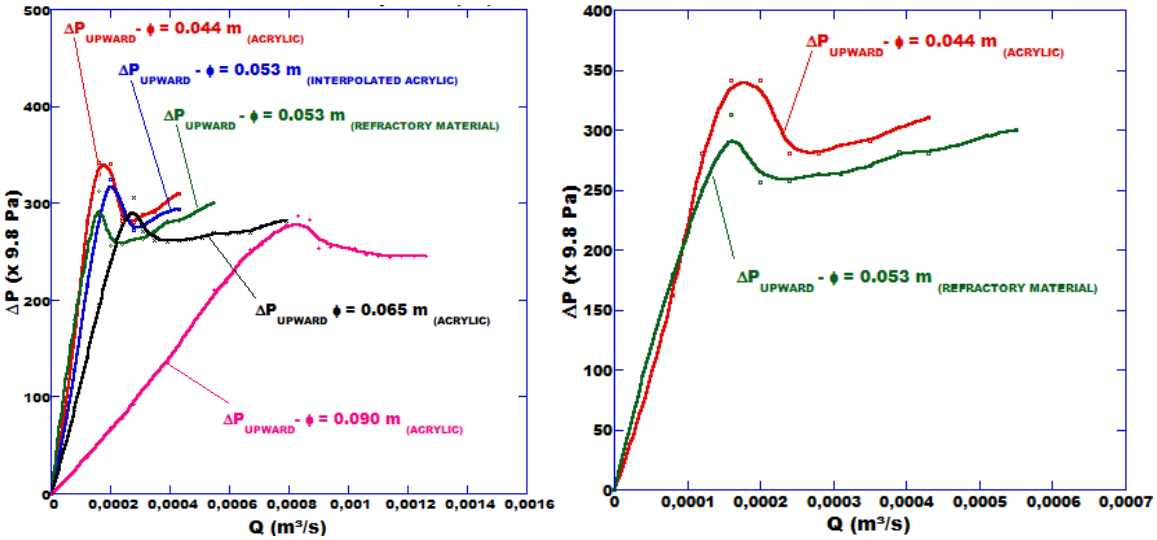

(a) (b)

Figure 7: (a) Graph of pressure profile ΔP x Q to different bed diameters - roughness effect, D_p=546 µm (Upward). (b) Graph of pressure profile ΔP x Q to ϕ = 0.053 m and ϕ = 0.044 m - roughness effect, D_p=546 µm (Upward).

Fig. 8 (a) shows results of fluid dynamics tests performed to investigate how the pressure drop is influenced by the increase in mean bed temperature where the thermocouple was installed at a reference position on the lateral of the reactor and 0.200 m above of base (T3). The fluidization of the silica was performed prior to starting the heating to avoid the exaggerated compaction effect as quoted previously. For each test with different mean initial bed temperatures, fluidization was initiated without compaction. This fact explains the absence of the peak of maximum pressure before the point of minimum fluidization, presented in the curves of this graph. As can be seen in Figure 8 (a), the slope relative to the fixed bed regime increases according to the growth of the mean reference temperature. Thus, this slope shows how the minimum air flow needed to fluidize the sand decreases with increasing temperature. These results were obtained with the following experimental conditions: ϕ = 0.053 m, initial bed height of 0.175 m, Dp = 546 µm, thermocouple at 0.200 m of the base. The slope of the "ΔP_{UPWARD} – T3 = 631°C" curve after fluidization shows the faster occurrence of the slugging regime and the reduction of the bubbling regime range. Thus, according to the presented data, it is verified that the slugging regime occurs for smaller flows as the average bed temperature increases.

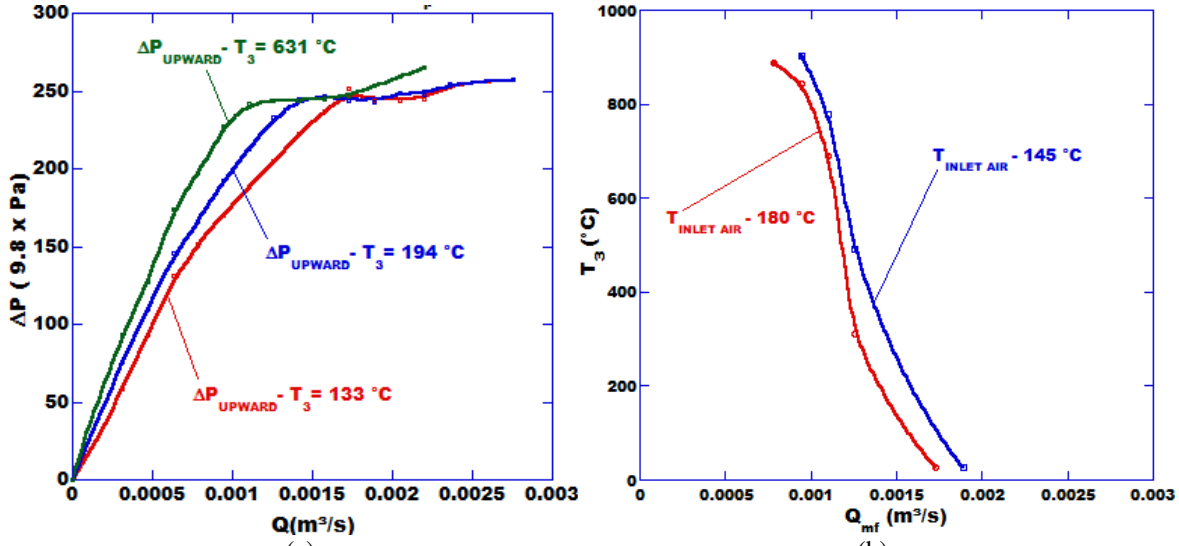

(a) (b)

Figure 8: (a) Graph of pressure profile ΔP x Q to different bed temperatures, D_p=546 µm and ϕ=0.053 m. (b) Graph of bed temperature profile T_3 x Q_{mf}, to different inlet air temperatures.

Fig. 8 (b) shows the results of fluid dynamics tests performed to study in detail how the minimum flow rate of fluidization is influenced by bed temperature for different inlet air temperatures. These tests were carried out under the following operating conditions: bed diameter of 0.053 m, bed initial quota of 0.175 m, average particle size of 546 µm, thermocouple at 0.200 m of the base (T3). These factors were kept constant while the temperature measurement was carried out and the point of the minimum fluidization was investigated for different average temperatures of the inlet

air. The curves of this graph show the temperature values of the bed at the reference position (T3) as a function of the flow necessary to fluidize the silica to the inlet air temperatures of 145 and 180 °C. By means of these experimental data, it is possible to notice that in a non-compacted bed, the minimum air flow of fluidization tends to decrease with the increase in bed temperature. In addition, it is observed that the increase of the inlet air temperature influences in the reduction of the minimum flow rate of fluidization required, however, the two curves show a same trend.

Fig. 9 (a) shows the temperature distribution profiles in the radial direction of the fluidized bed reactor, at a height (0.010 m) from the base. Figure 9 (b) also shows the temperature distribution profiles, but in the axial direction, along the length of the reactor and for the same conditions of operation. For the two profiles of these graphs it was employed an equivalence ratio of 1.19, resulting in characteristic curves. The highest one represents the temperature values shortly after the shutdown of the heating system that aided in the startup process of the FBR. The second curve, with a profile slightly lower than the first one, represents the temperature values 5 minutes after that of the supply of the air-fuel mixture to the startup system was interrupted. In the same way, the following curves, from top to bottom, represents the temperature values for subsequent instants as described in the graphs. Through the temperature distribution profiles, it has been found that the distance between successive curves decreases along the bed transient regime. The lowest curve, referring to the temperature distribution when a stable operating regime was achieved in the process of bubbling fluidized bed combustion. For the regions closest to the bed center, it is possible to observe the operation temperature between 800 and 900 °C. It is also possible to see in the graph of Fig. 9 (b) that the zone filled with sand is the most heated with respect to the freeboard zone of the reactor.

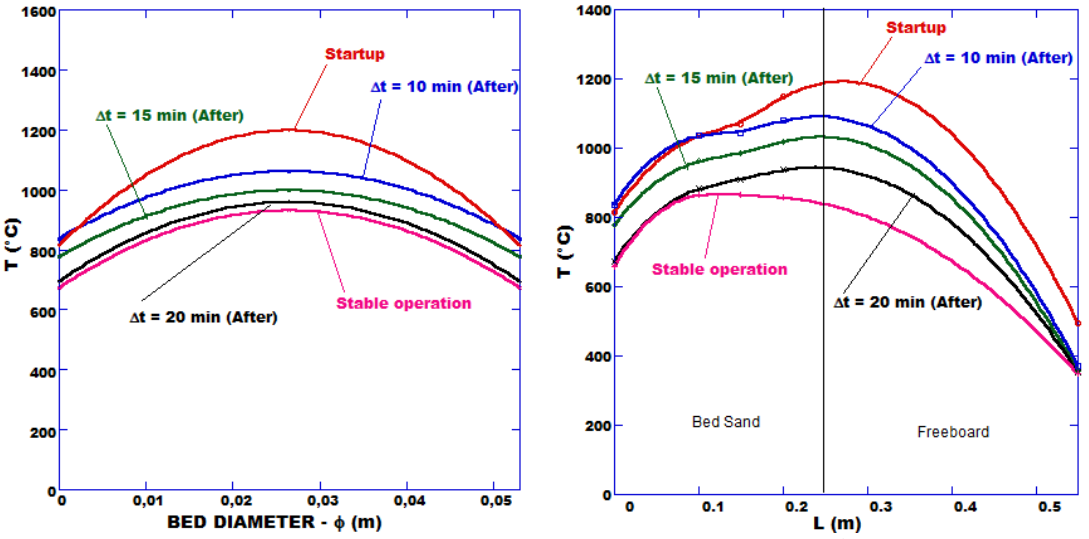

(a) (b)

Figure 9: (a) Graph of temperature profile T x ϕ, operation of the FBR with NG.
(b) Graph of temperature profile T x L, operation of the FBR with NG

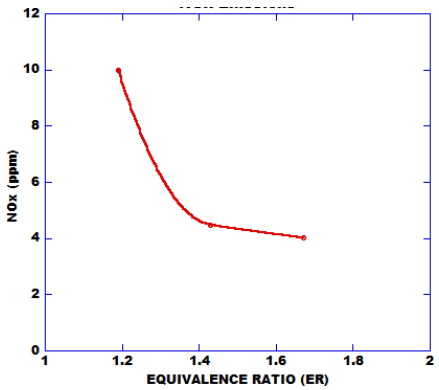

Figure 10: NOx emissions of the FBR with NG

Fig. 10 shows an NOx emission profile in which the study focused on the indices for slightly rich mixtures, in view of the majority of the studies have dealt with regions of poor mixtures. Thus, this work sought to evidence a possibility of biomass utilization in gasification processes and, for this reason, the reactor of fluidized bed was operated with mixtures slightly higher than stoichiometry of air with natural gas to obtain data for a comparative analysis with gasification in the same conditions in terms of equivalence ratio.

5. CONCLUSIONS

With this experimental investigation, some parameters were obtained that can support the development of a combustion fluidized bed reactor. Thus, some conclusions are enunciated:

• Relative similarities in fluid dynamics phenomena of the bed fluidization process between the silica of 546 μm and 321 μm allows the use of the sand with larger granulometry, because it has a lower cost.

• For different bed diameters with the same height, a higher fluid flow velocity is required for fluidization. In contrast, for larger bed diameters, the fluid flow range in bubbling fluid bed (BFB) regime is larger and more stable. This suggest the use of larger bed diameters to allow a wider range of fluid flow variation in the condition of BFB.

• Other important aspects were the operating temperature range of fluidized bed reactors between 800 °C and 900 °C, as NOx emissions in the FBR were low.

• It was observed the existence of an "optimal" operating quota suggested by the L/D ratio (L = bed length, D = bed diameter). Applying the L/D ratio in the three cases (225/44 = 5.1, 325/65 = 5.0, 425/90 = 4.7), a design parameter is identified, which can be adequate to BFB reactor development.

6. ACKNOWLEDGEMENTS

This work was supported by two Brazilian Government's Scientific and Technological Development Institutions: FUNCAP (Foundation of Ceara of Support to the Scientific and Technological Development) and CAPES (Coordination for the Improvement of Higher Education Personnel). Also, the BNDES (National Bank of Development) supported this research.

7. REFERENCES

Basu, P., 2006. Combustion and Gasification in Fluidized Beds. New York: Taylor & Francis Group.

Bisognin, P.C., Fusco, J.M. and Soares, P. C., 2016. Heat transfer in fluidized beds with immersed surface: Effect of geometric parameters of surface, Powder Technology 297. 401–408.

BP Energy Outlook 2035, 2015. BP p.l.C. London, United Kingdom, 64th edition (February).

BP Statistical Review of World Energy, 2015. BP p.l.C. London, United Kingdom, 64th edition (June).

Dounit, S., Hemati, M. and Andreux, R., 2008. Modelling and experimental validation of a fluidized-bed reactor freeboard region: Application to natural gas combustion, Chemical Engineering Journal 140. 457–465.

Dryer, F.L. and Glassman, I., 1973. High temperature oxidation of CO and CH4, in: Proceedings of the 14th International Symposium on Combustion, The Combustion Institute, Pittsburg, p. 987.

EIA, Energy Information Administration, 1999. Natural Gas 1998 Issues and Trends. Office of Oil and Gas. U.S. Department of Energy, Washington, DC, pp. 49e71, 20585, Ch.2.

Ergun, S., 1952. Fluid Flow Through Packed Columns. Journal of Chemical Engineering Progress, vol. 48, nº 2, pp. 1179-118.

Geldart, D., 1986. Gas Fluidization Technology. London: Wiley & Sons Ltd, 1986.

Ngoh, J. and Lim, E.W.C., 2016. Effects of particle size and bubbling behavior on heat transfer in gas fluidized beds, Applied Thermal Engineering 105. 225–242

Kunii, D. and Levenspiel, O., 1990. Fluidized reactor models: 1. For bubbling beds of fines, intermediate and large particles. 2. For the lean phase: freeboard and fast fluidization, Ind. Eng. Chem. Res. 29. 1226–1234.

Moreira, A. P. A.; Barcellos, W. M.; Feitosa, J. D. M. et al., 2013. Parametric Approach About Fluidized Bed Of Particles Of Silica And Cashew Nut Shell. 22th International Congress of Mechanical Engineering (Cobem), Ribeirão Preto, Sp, 2013. pp. 10013-10022.

Oka, S. N., 2004. Fluidized Bed Combustion. New York: Marcell Dekker.

Pré, P., Hémati, M. and Marchand, B., 1998. Study of natural gas combustion in fluidized beds: modelling and experimental validation, Chem. Eng. Sci. 53 (16) 2871.

Salatino, P. and Solimene, R., 2017. Mixing and segregation in fluidized bed thermochemical conversion of biomass, Powder Technology 316. 29–40.

Singh, R.I., Brink, A. and Hupa, M., 2013. CFD modeling to study fluidized bed combustion and gasification, Applied Thermal Engineering 52. 585–614.

Sotudeh-Gharebaagh, R., Chaouki, J. and Legros, R., 1999. Natural gas combustion in a turbulent fluidized bed of inert particles, Chemical Engineering Science 54. 2029–2037.

Zukowski, W., 2003. A simple model for explosive combustion of premixed natural gas with air in a bubbling fluidized bed of inert sand, Combustion and Flame 134. 399–409.

8. RESPONSIBILITY NOTICE

The authors are the only responsible for the printed material included in this paper.